ARTICLE

Low-Energy Electron Attachment to Serine Conformers: Shape Resonances and Dissociation Dynamics

Yongfeng Wang[a*], Shan Xi Tian[b]

a. Key Laboratory of Neutronics and Radiation Safety, Institute of Nuclear Energy Safety Technology, Chinese Academy of Sciences, Hefei 230031, China
b. Hefei National Laboratory for Physical Sciences at the Microscale and Department of Chemical Physics, University of Science and Technology of China, Hefei 230026, China

(Dated: Received on December 19, 2016; Accepted on February 13, 2017)

Shape resonances of electron-molecule system formed in the low-energy electron attachment to four low-lying conformers of serine (serine 1, serine 2, serine 3, and serine 4) in gas phase are investigated using the quantum scattering method with the non-empirical model potentials in single-center expansion. In the attachment energy range of 0−10 eV, three shape resonances for serine 1, serine 2, and serine 4 and four shape resonances for serine 3 are predicted. The one-dimensional potential energy curves of the temporary negative ions of electron-serine are calculated to explore the correlations between the shape resonance and the bond cleavage. The bond-cleavage selectivity of the different resonant states for a certain conformer is demonstrated, and the recent experimental results about the dissociative electron attachment to serine are interpreted on the basis of present calculations.

Key words: Serine, Conformational effect, Shape resonance, Dissociative electron attachment

I. INTRODUCTION

Low-energy electrons produced in the ionization radiation can lead to fragmentation of the surrounding molecules in biological tissues via electron resonant attachment [1]. The highly reactive radicals and anionic fragment could cause further chemical reactions or damages to system [1–8]. This electron-induced fragmentation process is known as dissociative electron attachment (DEA), in which the temporary negative ion (TNI) formed in the electron resonant attachment, as the predissociative short-lived intermediates, is theoretically classified into electron-molecule shape and Feshbach resonances [9]. Shape resonance as the simplest case is formed by trapping the excess electron in a potential well of the neutral molecule, in which the potential barrier is the combined effect of the attractive polarization potential and the repulsive centrifugal potential. Shape resonances were frequently observed in the electron attachment to nucleic acid bases and amino acids. These shape resonances are believed to play very important roles in the DEA to biomolecules, particularly in the lower attachment energy range (*i.e.*, less than 10 eV) [1, 6, 10–13].

Lots of experimental studies on the DEAs to isolated biomolecules and the building blocks of DNA/RNA and proteins have been performed in the last decades [14–24]. Theoretical approaches of low-energy electron scattering of uracil [13, 25, 26], formic acid [27, 28], and glycine [27, 29–31] were made by using quantum scattering methods, such as the non-empirical model potentials in a symmetry-adapted, single-center expansion (SCE) and the R-matrix method. In addition, the Schwinger multichannel method was applied by Winstead and McKoy for nucleobases and other DNA constituents [32–34]. The possible mechanisms of DNA-strand breaks induced by low-energy electrons were also discussed by Simons *et al.* using electronic structure theory [5, 6]. Recently, the dissociative dynamics simulations of the sugar backbones [35], formamide [36], and amino acids [37] were carried out by Gianturco *et al.* using quantum scattering method together with one-dimensional (1D) modeling for the dissociative dynamics. It should be noted that most theoretical studies focused on the lowest-energy conformers, except for the glycine conformers [29] and the tautomers of nucleic acid bases [38]. In the gas-phase experiments, several low-lying stable conformers or tautomers usually coexist [39–46]. Therefore, it is important to reveal whether or how the conformers or tautomers influence the electron-molecule resonant states and the subsequent dissociation dynamics. In our previous work [38], the tautomeric effect on the shape resonances of nuclear acid bases was observed clearly.

In the present work, the shape resonances formed in the low-energy electron attachment to four low-lying

*Author to whom correspondence should be addressed. E-mail: yongfeng.wang@fds.org.cn

conformers of serine (serine 1, serine 2, serine 3, and serine 4, as depicted in Fig.1) and the subsequent dissociation dynamics are investigated with the non-empirical model potentials in SCE. It has been confirmed that the four conformers could coexist in the gas phase [45, 46]. Recently, the DEA to the gas-phase serine was also studied by using the electron-molecule cross beam technique [24]. Here we not only focus on the conformer effects on the DEA to serine, but also explore the bond-cleavage selectivity of the different resonant states for a certain conformer. The later mechanism has been demonstrated in our previous studies on the resonant DEAs to the lowest-lying conformers of cysteine and cystine [47].

II. THEORETICAL METHODS

In contrast to the anionic biomolecules in solutions where the solute-solvent interaction can stabilize the excess electron, the gas-phase TNI formed by the electron attachment is short-lived because its resonant states strongly couple with the electron continuum. Several quantum scattering methods [26, 34, 48, 49] can properly elucidate the formation of TNIs in gas phase. Here we use the SCE method which has been successfully applied in the studies of the DEAs both to DNA bases [13, 25, 38] and amino acids [28–30, 47]. Since the theoretical details of SCE scattering method are available [49], we only review some main points.

The equilibrium structures of the four low-lying energy serine conformers are optimized at MP2/6-311++G(d,p) level. The electron wave function of molecular orbital (MO) is given in the self-consistent field approximation with a single-determinant description (static exchange approximation). Then the wave functions of both the bound and the continuum electrons are expanded at the center of mass of the target (*i.e.*, SCE) by employing symmetry-adapted angular functions with their corresponding radial coefficients represented on a numerical grid [49]. Any arbitrary three-dimensional single-electron function $F(r)$ is determined with the scattering equation,

$$\left[\frac{1}{2}\nabla^2+(E-\varepsilon)\right]F(r)=\int V(r,r')F(r')\mathrm{d}r' \qquad (1)$$

where E=$k^2/2$ is the collision energy and ε is the electronic eigenvalue of the target. The integral operator V includes the electrostatic (V^{st}) interaction and exact nonlocal exchange interaction for a single state, as well as a supplementary term V^{cp} for the electron correlation and long-distance polarization effects. V^{cp} can be introduced both with the Perdew-Zunger correlation V^{corr} [50] and the polarizability tensor function V^{pol},

$$V^{\mathrm{pol}}=-\frac{1}{2r^6}\sum_{i=1}^{3}\sum_{j=1}^{3}q_iq_j\alpha_{ij} \qquad (2)$$

where α_{ij} are six terms of the polarizability tensor and $q_{i,j}$=x, y, z. All of the molecular properties and equilibrium structures used in the scattering calculations are predicted with Gaussian 09 program [51]. Furthermore, the exact nonlocal bound-continuum exchange interaction considered in Eq.(1) is replaced with free-electron-gas exchange (FEGE) potential as proposed by Hara [52, 53],

$$V_{\mathrm{FEGE}}=\frac{2}{\pi}k_{\mathrm{F}}(r)\left(\frac{1}{2}+\frac{1-\eta^2}{4\eta}\ln\left|\frac{1+\eta}{1-\eta}\right|\right) \qquad (3)$$

where k_{F} is the Fermi momentum and η is the neutral's ionization potential. Thus the scattering Eq.(1) can be rewritten in the static model exchange correlation polarization approximation,

$$\left[-\frac{1}{2}\nabla^2-\frac{1}{2}k^2+\hat{V}^{\mathrm{st}}+\hat{V}^{\mathrm{cp}}+\hat{V}^{\mathrm{FEGE}}\right]F(r)=0 \qquad (4)$$

The local formulation can be cast in terms of the usual partial wave expansion. After integrating over the angular, K-matrix elements can be derived. Then a set of partial wave phase-shifts $\delta_l(k)$ for S-matrix elements S_l=$S_l(k)$=$\mathrm{e}^{2i\delta l(k)}$ are obtained for all the contributing angular momenta. The position E_{res} and width Γ_{res} of a resonant state can be determined in the search for poles of the S-matrix [49]. In this work, the poles of the S-matrix are calculated using more than 200 radial regions for the four lowest energy serine conformers, including the piecewise diabatic potential terms up to l=12. The radial integrations are carried out in the 18.0 Å regions. The D95** basis set is employed to generate the target wave functions. The calculations of the potential are carried out up to l=80 for the initial multipolar expansion and the scattering wave functions included partial waves up to l_{max}=40. The scattering calculations are performed with the ePolyScat.E2 program [54, 55].

In the electron attachments, the surplus energy after attachment must be dissipated, *e.g.*, via intramolecular vibration redistribution (IVR). The redistribution processes can be simply simulated with 1D calculations, *i.e.* inspecting the shifts of the calculated E_{res} and Γ_{res} values along a certain bond stretching [35–37],

$$E_{\mathrm{tot}}(R)=E_{\mathrm{res}}(R)+E_N(R)-E_N(R_{\mathrm{eq}}) \qquad (5)$$

where $E_N(R)$ is the electron energy of the neutral molecule (N-electron target) at a set of geometries (here a scanning step is 0.2 Å) and $E_N(R_{\mathrm{eq}})$, as a reference, is the energy at the equilibrium geometry. The 1D complex potential energy modeling mimics whether the bond stretching at a certain state is directly responsible for the decompositions of TNI. The resonant state [(N+1)-electron system] at each stretching geometry has,

$$E_{\mathrm{res}}^{\mathrm{complex}}(R)=E_{\mathrm{res}}(R)-i\frac{\Gamma_{\mathrm{res}}(R)}{2} \qquad (6)$$

DOI:10.1063/1674-0068/30/cjcp1612228

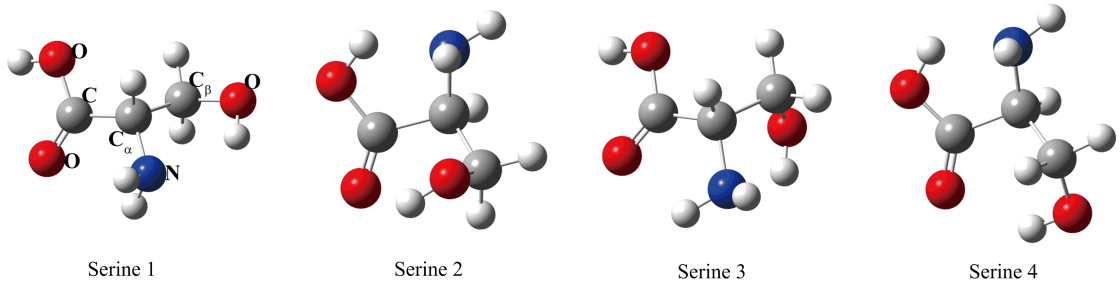

FIG. 1 Equilibrium structures of the four low-lying energy serine conformers.

TABLE I Energies (E_{res}) and widths (Γ_{res}) of the resonant states in the low-energy electron attachment to the four low-lying serine conformers.

	Serine 1		Serine 2		Serine 3		Serine 4	
State	E_{res}/eV	Γ_{res}/eV	E_{res}/eV	Γ_{res}/eV	E_{res}/eV	Γ_{res}/eV	E_{res}/eV	Γ_{res}/eV
1	2.68	0.15	3.28	0.31	3.04	0.28	3.16	0.40
2	8.88	1.09	8.23	2.53	8.62	2.44	7.74	1.05
3	9.88	1.28	8.26	1.47	8.97	2.51	9.49	2.83
4					9.88	2.18		

III. RESULTS AND DISCUSSIONS

A. Shape resonances

The equilibrium structures of the four low-lying conformers (serine 1, serine 2, serine 3, and serine 4) are depicted in Fig.1. According to the present calculations, the relative energies with respect to serine 1 are 0.17, 1.47, and 4.04 kJ/mol for serine 2, serine 3, and serine 4, respectively. The relative stability predicted in the present work is consistent with that proposed by Alonso *et al.* [45] at the MP4/6-311++G(d,p)//MP2/6-311++G(d,p) level, but the relative energies are slightly different. The stability order predicted here is different from that proposed by Maes *et al.* [46] at the B3LYP/6-311++G(d,p) level. This difference should be due to the different levels of theory used in the calculations. In the present work, we do not pay more attention to the relative stabilities of the serine conformers, since these conformers have been proven to coexist in the gas-phase experiments [45, 46].

In Table I, the shape resonant energies together with the respective widths are listed. For serine 1, serine 2, and serine 4, three resonant states are predicted at the electron attachment energies less than 10 eV, while four states for serine 3. In the experimental studies [11, 56], π^* and σ^* were frequently employed in the assignments to the resonant states for the TNIs of amino acids. In the present work, these states are renamed according to their energetic sequence, because there are no molecular symmetric planes. However, the localized character of the resonant wave function still needs to be emphasized, for instance, a pseudo-π^* state can be formed in the electron attachment to serine due to the significantly local π^* (COOH) orbital character of the resonant wave function (see the resonant wave functions of states 1 for the four conformers in Fig.2). To the best of our knowledge, there are no theoretical studies prior to this work about the positions of shape resonances of serine. For the first resonant states of the four conformers, the resonant wave functions show the similar characters (see Fig.2), belong to pseudo-π^* state. However, state 1 for serine 1 is predicted at 2.68 eV with width of 0.15 eV, while, for serine 2, serine 3, and serine 4, the resonant energies of states 1 shift to more than 3 eV and the widths become larger. This implies that the excess electron may be more easily captured by serine 1. The differences in the energies and widths of the first resonant states indicate that the conformational effect exists for the four serine conformers. For the resonant states at the higher energies, the conformational effect in resonant energies and widths is more distinct (as shown in Table I). Such as, the resonant energy of state 2 for serine 4 is 7.74 eV, while the resonant energies of states 2 for the other three conformers are higher than 8.0 eV.

The conformational effect is also shown clearly in the resonant wave functions. As depicted in Fig.2, the wave functions of states 2 for serine 1, serine 2, and serine 4 and of state 3 for serine 3 show similar characters. Their anti-bond characters in the $C_\alpha-N$ and $C_\beta-OH$ bonds are clearly visualized as the nodal planes. For state 3 of serine 1, there are nodal planes perpendicular to the $C_\alpha-C$, $C-OH$, $C_\alpha-NH_2$, and $C_\beta-OH$ bonds. For state 3 of serine 2, there are nodal planes perpen-

DOI:10.1063/1674-0068/30/cjcp1612228

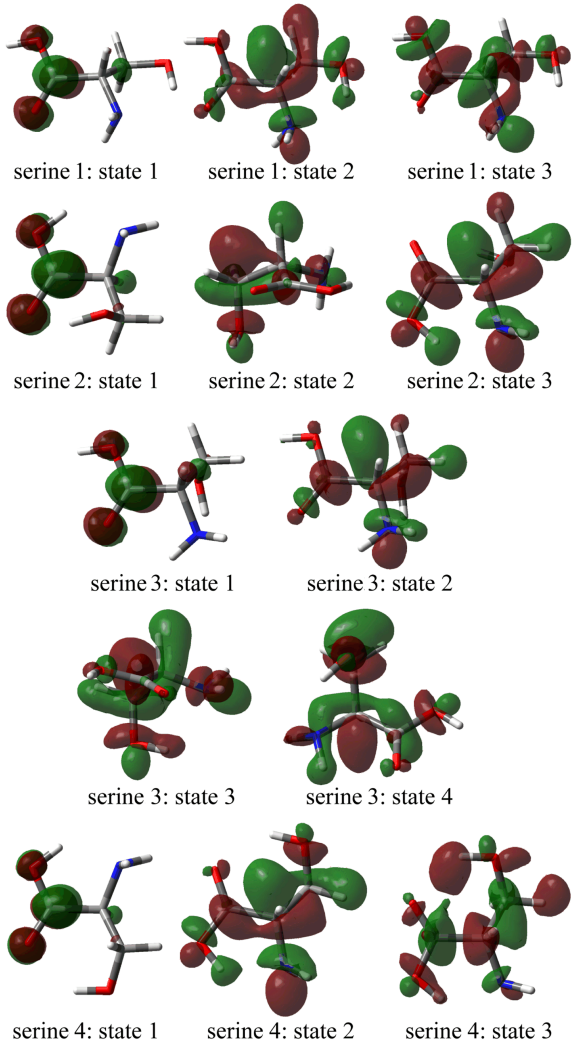

FIG. 2 The resonant electron wave functions of the resonant states for serine 1, serine 2, serine 3, and serine 4 at the equilibrium structures.

dicular to the $C_\alpha-C$, C−OH, and $C_\alpha-NH_2$ bonds. For state 2 of serine 3, the nodal planes localize at the $C_\alpha-C$ and $C_\alpha-NH_2$ bonds. For state 3 of serine 4, there is only one nodal plane perpendicular to the $C_\alpha-C$ bond. For state 4 of serine 3, the anti-bond character clearly shows for the $C_\alpha-C_\beta$ bond. Therefore, the conformational effect is very remarkable in low electron attachment energy range.

Since the TNIs are usually regarded as the precursors of DEA, the subsequent DEA channels could be deduced preliminary according to the characters of the resonant wave functions. However, caution must be exercised to derive conclusions because this involves a certain degree of speculation. On the other hand, one needs to be circumspect about the shape resonant states at the higher energies. For the energy higher than electron excitation or ionization thresholds, Feshbach resonances and their couplings with shape resonances should be considered. In the present work, the electron excitations of the target molecule are not included, therefore, Feshbach resonances are not considered. Here a remarkable relationship between the shape resonant state and the bond cleavage will be established by analyzing the 1D potential energy curves.

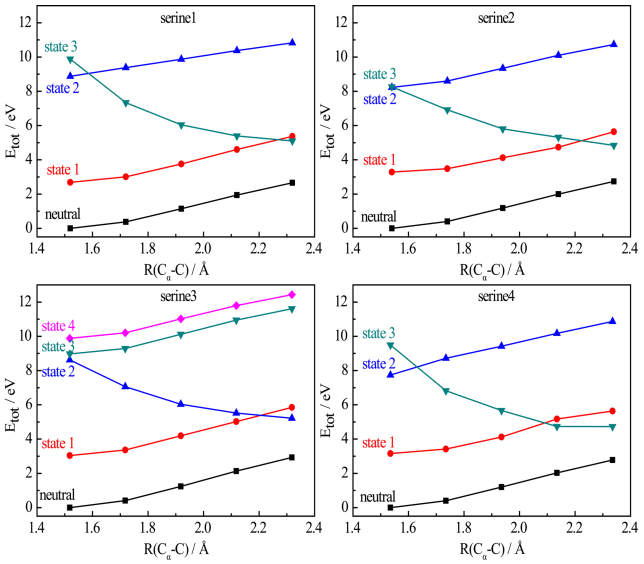

FIG. 3 Total electronic energy changes of the neutral and shape resonances along the $C_\alpha-C$ stretching coordinate for serine 1, serine 2, serine 3, and serine 4.

B. One-dimensional dissociation dynamics

The 1D complex potential energy modeling will be used to simulate the dissociation of the TNIs at each resonant state and the dissociation mechanism about the DEA experimental observations [24] could be elucidated. Although the full-dimensions complex potential surface could explain the dissociation processes comprehensively, the calculations are more computationally expensive. In the present work, the 1D potential energy curves along $C_\alpha-C$, $C_\alpha-C_\beta$, $C_\alpha-N$, $C_\beta-OH$, and C−OH bonds will be calculated. The conformational effects on the dissociative dynamics will also be emphasized.

1. 1D dissociation dynamics along $C_\alpha-C$ bond stretching

The 1D potential energy curves of the shape resonances for the four conformers along the $C_\alpha-C$ stretching coordinate (Fig.3) are predicted with Eq.(5), where the $C_\alpha-C$ bond is elongated gradually in the plane of $C_\alpha-C-OH$ while the residual parts are fixed at the equilibrium geometries. During the $C_\alpha-C$ bond elongations, the total electronic energy curves of states 3 for serine 1, serine 2, and serine 4 and state 2 for serine 3 gradually decrease and cross with the curves of

DOI:10.1063/1674-0068/30/cjcp1612228

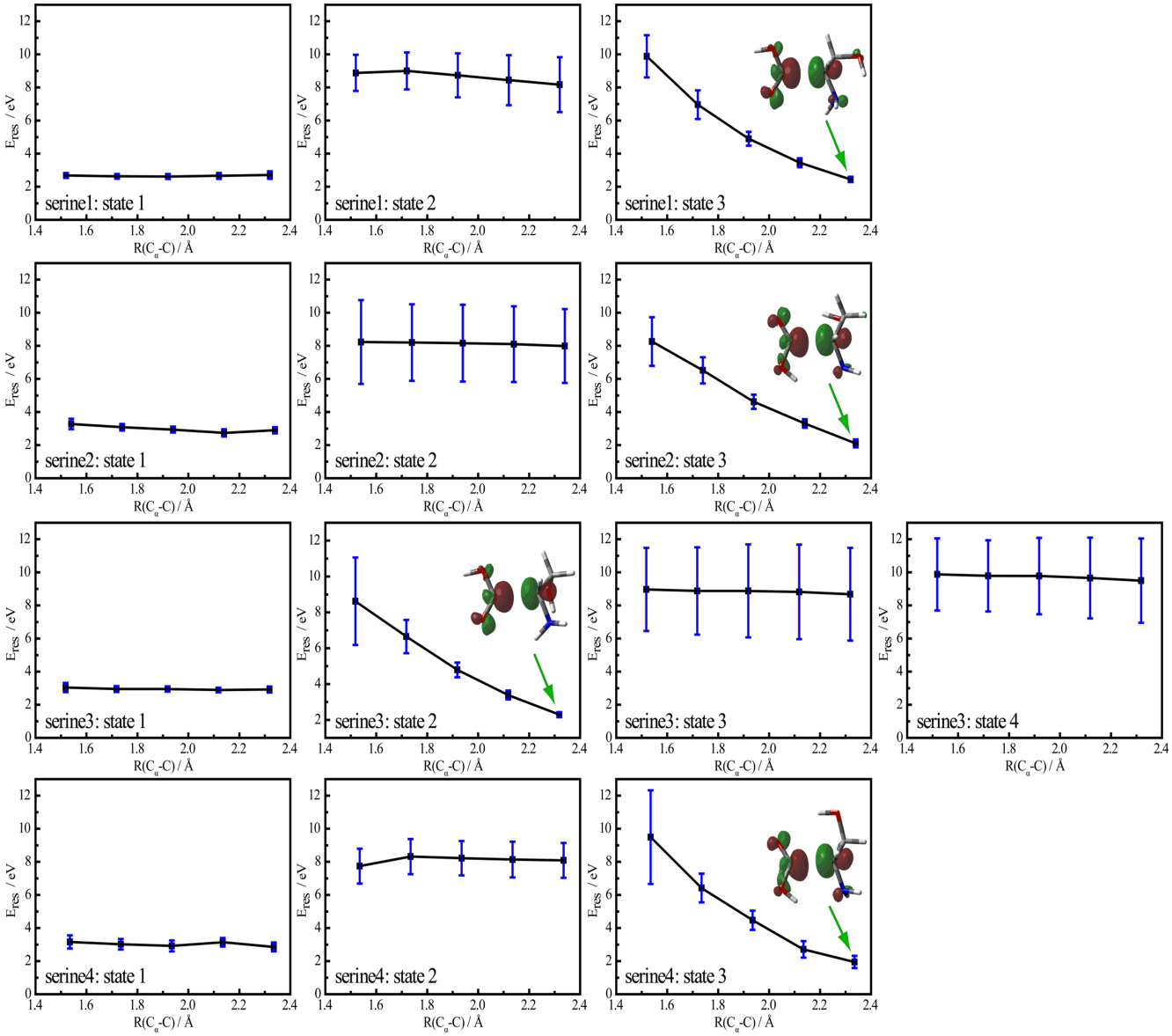

FIG. 4 Resonant energy changes of the shape resonances along the $C_\alpha-C$ stretching coordinate for serine 1, serine 2, serine 3, and serine 4. The insets indicate the resonant electron wave functions of the associated resonant state. The error bars report the widths of the associated resonant states. Wave functions are plotted with contour values of ± 0.15 a.u.

states 1 for the four serine conformers. The crossing points imply that there may be conical intersections of the potential energy surface between these two states. The total energies of the other resonant states are found increasing along the $C_\alpha-C$ bond stretching.

In Fig.4, the complex potential energies at each resonant state are plotted in terms of the selected bond elongations (using Eq.(6)). When the $C_\alpha-C$ bond is elongated, both the resonant energies $E_{\rm res}$ and widths $\Gamma_{\rm res}$ of states 3 for serine 1, serine 2 and serine 4 and state 2 for serine 3 dramatically decrease. The decrease of $\Gamma_{\rm res}$ means that the TNIs at these resonant states become more and more stable with the $C_\alpha-C$ bond stretching. In the resonant wave function maps, the nodal plane across the $C_\alpha-C$ bond becomes much clearer. All of above imply that the direct cleavage of $C_\alpha-C$ bond is favorable both in energy and in dynamics for TNIs at these resonant states.

When the $C_\alpha-C$ bond length increases by 0.8 Å, the resonant electron wave functions of the resonant states with the decreasing $E_{\rm res}$ values are mainly distributed on the $C_\alpha-C$ bond. The nodal plane across the $C_\alpha-C$ bond gradually becomes clearer (see the insets in Fig.4). All of the above indicate that TNIs at these resonant states could play important roles in production of $COOH^-$ or $(serine\text{-}COOH)^-$ anionic fragments by the $C_\alpha-C$ bond cleavage. In recent DEA experiments on serine [24], $COOH^-$ negative ions were detected in

DOI:10.1063/1674-0068/30/cjcp1612228

the electron energy range of 4−10 eV, and the peak value appears to be at around 5.5 eV in the anionic yield curves. However, in the present work, the resonant energies of states 3 for serine 1 (9.88 eV), serine 2 (8.26 eV) and serine 4 (9.49 eV) and state 2 for serine 3 (8.62 eV) are higher than 5.5 eV. In the present calculation, the model searches for the resonances as initially being shape resonances and employs a model treatment of exchange and polarization interactions [25, 49–53]. Although there are no empirical parameters in our calculations, the above forces are certainly approximate and therefore they will shift the resonances from their exact positions. The previous theoretical results also show about 1−2 eV energy shifts to higher values for the low-energy shape resonances, especially for the π^* or pseudo-π^*resonances [12, 38]. For high-energy resonances, the mismatch will become larger. Therefore, the resonant states could be possible as precursor states to $COOH^-$ fragments observed in the energy region of 4−10 eV, and the peak value appears to be at around 5.5 eV in the DEA experiment [24]. Moreover, the $(serine\text{-}COOH)^-$ negative ion with mass of 60 amu was not detected in the DEA experiment. In our calculations, we could not exclude the formation of $(serine\text{-}COOH)^-$ ions.

In Fig.4, the flat curves of states 1 and 2 for serine 1, serine 2, and serine 4 and states 1, 3, and 4 for serine 3 indicate that the C_α−C bond cannot be spontaneously broken at these states. But the crossing points observed in Fig.3 indicate that the C_α−C bond could be potentially broken after the resonant state transition through the conical intersection. It is noted that there are nodal planes in the C_α−C bonds in the wave functions of state 4 for serine 3 and state 2 for serine 4 (see Fig.2), however, the total electronic energies of the two states increase and the resonant energies and widths do not decline when the C_α−C bond is elongated (see Fig.3 and Fig.4), which indicate that C_α−C bond will not be broken when the TNIs at these resonant states. Therefore, caution must be exercised to derive DEA conclusions using the nodal planes in the resonant wave functions.

2. 1D dissociation dynamics along C_α−C_β bond stretching

Serine is an aliphatic amino acid and contains a CH_2OH group in the side chain. In the present work, the 1D dissociation dynamics along C_α−C_β bond stretching is calculated to investigate the dissociation process of the side chain. Total electronic energy changes of the neutral and shape resonant states along the C_α−C_β stretching coordinate for serine 1, serine 2, serine 3, and serine 4 are shown in Fig.5. The total electronic energy of state 4 for serine 3 decreases dramatically. As the C_α−C_β bond length increases by 0.2 Å, some new resonant states (named state 4) appear for serine 1, serine 2, and serine 4 whose total

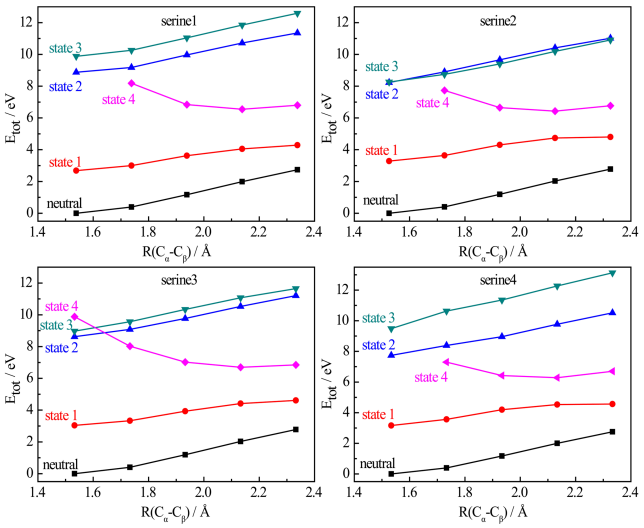

FIG. 5 Total electronic energy changes of the neutral and the shape resonances along the C_α−C_β stretching coordinate for serine 1, serine 2, serine 3, and serine 4.

electronic energies, resonant energies, and widths also decrease during the C_α−C_β stretching. From the resonant wave functions of states 4 for the four serine conformers (see the insets in Fig.6), one could find that as the C_α−C_β bond length increases by 0.8 Å, the charge is mainly localized at $(serine\text{-}CH_2OH)^-$ part. All of the above imply that TNI at state 4 for serine 3 could induce the C_α−C_β cleavage directly, thereby leading to $(serine\text{-}CH_2OH)^-$ fragments but not the CH_2OH^-. In the recent DEA experimental study [24], a large number of $(serine\text{-}CH_2OH)^-$ fragments were detected in the energy range of 4−8 eV, and the CH_2OH^- fragment was not found. The present results are generally in agreement with DEA experiments. Since state 4 is not predicted in the energy range of 0−10 eV for serine 1, serine 2, and serine 4 at equilibrium structures, we suspect that the $(serine\text{-}CH_2OH)^-$ fragments detected in DEA experiment possibly come only from serine 3.

3. 1D dissociation dynamics along C_α−N, C_β−OH, and C−OH bond stretching

In recent DEA experiment, the negative fragment with mass of 16 amu was found [24]. The masses of O^- and NH_2^- are very close to 16 amu, thereby it is difficult to distinguish these two fragments in experiment. The O^- fragment likely comes from -OH group rather than via the C=O bond breakage, because the C=O bond strength is relatively high. For serine, the C_β−OH and C−OH bonds breakage could produce OH group and the C_α−N bond breakage could produce NH_2 group. Therefore, in the present work, the 1D dissociations along C_α−N, C_β−OH, and C−OH bond stretching are simulated in order to identify the possible source of the fragment with mass of 16 amu, in particular, the

DOI:10.1063/1674-0068/30/cjcp1612228

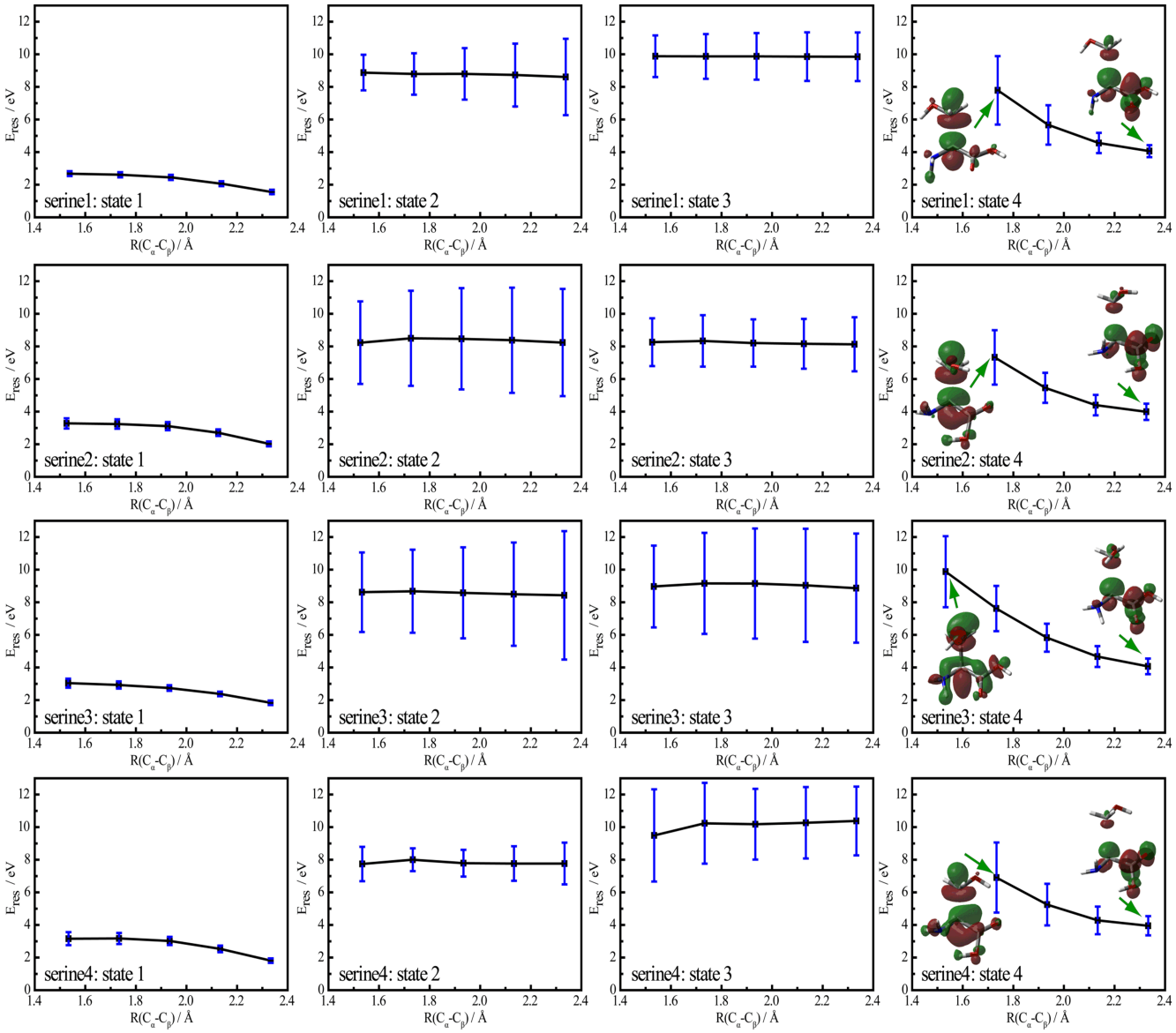

FIG. 6 Resonant energy changes of the shape resonances along the $C_\alpha-C_\beta$ stretching coordinate for serine 1, serine 2, serine 3, and serine 4. The insets indicate the resonant electron wave functions of the associated resonant states. The error bars report the widths of the associated resonant states. Wave functions are plotted with contour values of ±0.15 a.u.

role of the side -OH chain of serine.

The total electronic energies, resonant energies, and widths of states 2 for serine 1, serine 3, and serine 4 and state 3 for serine 2 are found to decrease when the $C_\alpha-N$ bond is elongated (see Fig.7 and Fig.8). Moreover, as shown in Fig.7, the total electronic energy curves of these resonant states cross with the curves of states 1 for the four serine conformers. According to the changes of the resonant wave functions, one could find that as the $C_\alpha-N$ bond length increases by 0.8 Å, the negative charge is mainly localized at $C_\alpha-N$ bond and the nodal plane on $C_\alpha-N$ bond becomes clear. Therefore, states 2 for serine 1, serine 3, and serine 4 and state 3 for serine 2 could induce the direct cleavage of $C_\alpha-N$ bond, thereby forming NH_2^- or $(\text{serine-NH}_2)^-$ fragments. Moreover, the TNIs at states 1 for the four serine conformers could also induce the $C_\alpha-N$ bond cleavage indirectly through the conical intersections.

The total electronic energies of states 2 for serine 1, serine 2, and serine 4 and state 3 for serine 3 are found to decrease with the elongation of the $C_\beta-OH$ bond. The energy curves of these resonant states also cross with that of states 1 (see Fig.9). Furthermore, as depicted in Fig.10, the energies and widths of states 2 for serine 1, serine 2, and serine 4 and state 3 for serine 3 also decreasing along $C_\beta-OH$ bond stretching, which indicates that direct cleavage of $C_\beta-OH$ bond is favorable both in energy and in dynamics for TNIs at these

DOI:10.1063/1674-0068/30/cjcp1612228

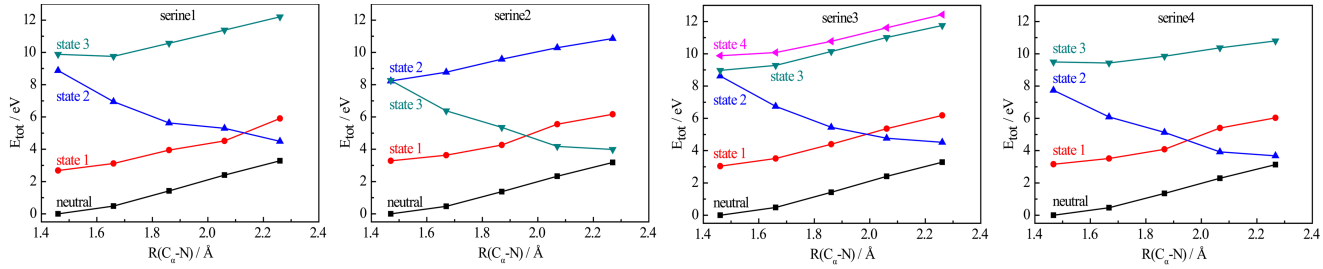

FIG. 7 Total electronic energy changes of the neutral and shape resonances along the $C_\alpha-N$ stretching coordinate for serine 1, serine 2, serine 3, and serine 4.

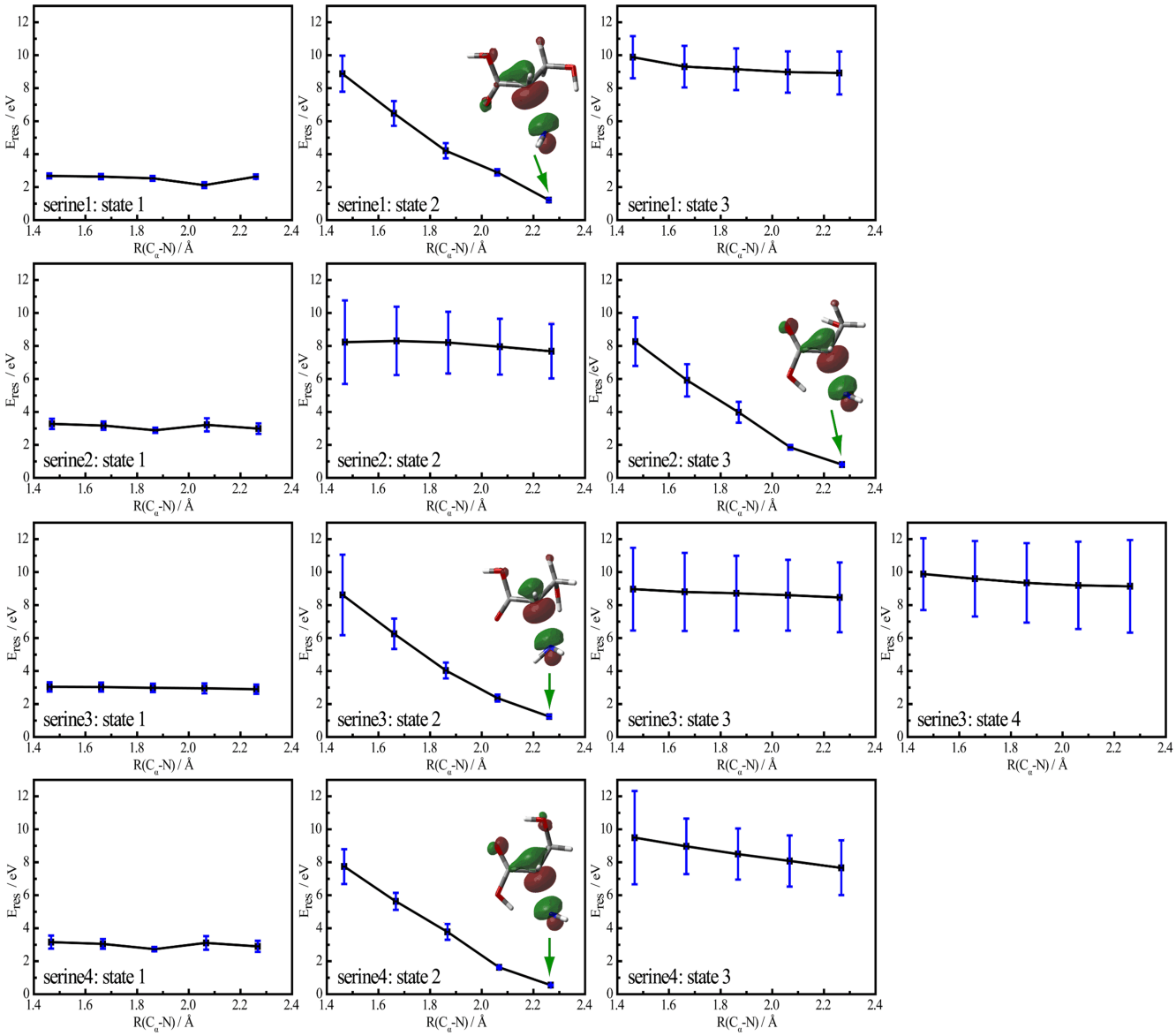

FIG. 8 Resonant energy changes of the shape resonant states along the $C_\alpha-N$ stretching coordinate for serine 1, serine 2, serine 3, and serine 4. The insets indicate the resonant electron wave functions of the associated resonant states. The error bars report the widths of the associated resonant states. Wave functions are plotted with contour values of ± 0.15 a.u.

DOI:10.1063/1674-0068/30/cjcp1612228

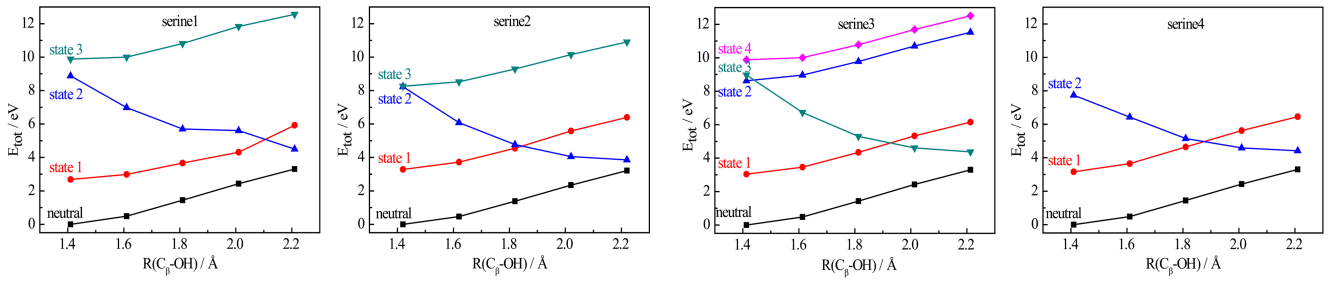

FIG. 9 Total electronic energy changes of the neutral and shape resonances along the $C_\beta-OH$ stretching coordinate for serine 1, serine 2, serine 3, and serine 4.

resonant states. Moreover, because the existence of conical intersections, TNIs at states 1 for the four conformers could decay through the $C_\beta-OH$ cleavage indirectly if these TNIs overcome the potential barrier. The wave functions of these resonant states show that along the $C_\beta-OH$ bond stretching the charge is localized on the $C_\beta-OH$ bond gradually. When the $C_\beta-OH$ bond length increases by 0.8 Å the distribution of negative charge is both on C_β atom and OH group. Therefore one could guess that the OH^- (O^-) or (serine-OH)$^-$ fragments could be produced during the dissociation of TNIs. In the DEA experiment [24], the two fragments were detected, but they were mainly found in the energy range of 0−2 eV. Firstly, other types of resonance may play more important role in the energy range of 0−2 eV, such as the vibrational Feshbach resonance. Secondly, the first resonant states (pseudo-π^* resonant state) may induce the $C_\beta-OH$ bond cleavage indirectly through the conical intersections. Some approximate methods are used in the present calculations, therefore the energies of the pseudo-π^* resonant states are larger than 2 eV. Therefore, we guess that vibrational Feshbach resonance and the first shape resonance may play very important roles for the fragments observed in the energy range of 0−2 eV. Moreover, it should be noted that there is a nodal plane on the $C_\beta-OH$ bond in wave function of state 3 for serine 1, but the 1D dissociation dynamics calculation indicates that the TNI at state 3 for serine 1 will not decay through the $C_\beta-OH$ bond cleavage directly.

For C−OH bond in the carboxyl group, the total electronic energies, the resonant energies, and widths for the shape resonant states along the C−OH bond stretching coordinate (as shown in Fig.11 and Fig.12) all indicate that TNIs at states 3 for serine 1 and serine 2 and at state 2 for serine 4 will decay by breaking the C−OH bonds directly. When the C−OH bond length increases by 0.8 Å, the distribution of charge on the (serine-OH) group becomes more than that on the OH group, which means that the probability of forming (serine-OH)$^-$ fragments is larger than that of forming OH^- anions.

Comparing $C_\beta-OH$ and C−OH bonds, we could find that the two bonds could be broken directly when the TNIs are at some special resonant states, thereby forming OH^- or (serine-OH)$^-$ fragments. The results of the present calculations indicate that the OH^- fragments mainly come from the side chain ($C_\beta-OH$ bond), because of the following reasons: (i) when the C−OH bond is broken, the probability of forming (serine-OH)$^-$ fragments is larger that of forming OH^- anions; (ii) the TNIs for serine 3 will not induce the cleavage of C−OH bond directly; (iii) the TNIs at state 1 for the four serine conformers could decay by breaking the $C_\beta-OH$ bond through the conical intersections indirectly, however, the conical intersection has not been found in the total electronic energies along C−OH stretching coordinate. Therefore, we guess that OH^- fragments observed in the DEA experiment mainly come from the side chain.

About the fragments with mass of 16 amu observed in the DEA experiment [24], from the calculations of 1D dissociation dynamics along $C_\alpha-N$, $C_\beta-OH$, and C−OH bond stretching, it is possible to produce NH_2^- or OH^- anions through the shape resonances calculated in the present work. Since O^- fragment likely comes from -OH group, it is possible to produce NH_2^- or O^- anions through the shape resonances. Therefore, we guess that the two anions could coexist in the DEA experiment. The fragments with mass of 16 amu were mainly observed in the energy regions of 0−2 and 6−9 eV in the DEA experiment [24]. Considering the approximation used in the present model, these shape resonant states could possible be as precursors to NH_2^- or O^- anions produced in the energy regions of 0−2 and 6−9 eV.

From the above analysis, one could find that conformational effect on the dissociation dynamics is also very clear. Such as, for the production of $COOH^-$ fragments, the resonances which could decay and form $COOH^-$ fragment are around 8.5 eV for serine 2 and serine 3. While for serine 1 and serine 4, the resonances which could decay and form $COOH^-$ fragment are around 9.5 eV. This means that in the DEA experiment, the $COOH^-$ fragments observed in lower energy range come from serine 2 and serine 3 and in higher energy range come from serine 1 and serine 4. Moreover, for serine 3, the TNIs could not decay through the C−OH bond

DOI:10.1063/1674-0068/30/cjcp1612228

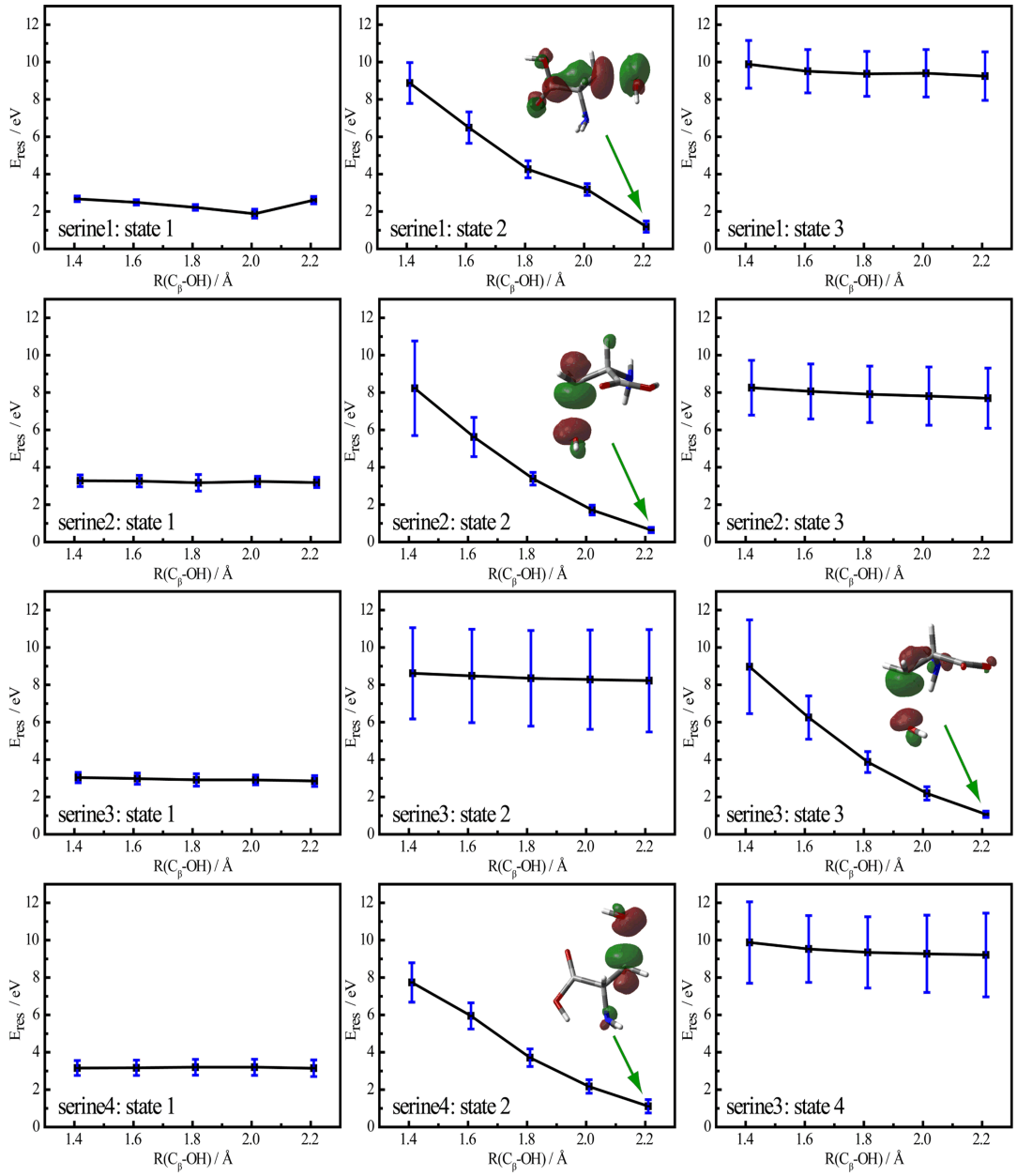

FIG. 10 Resonant energy changes of the shape resonant states along the $C_\beta-OH$ stretching coordinate for serine 1, serine 2, serine 3, and serine 4. The insets indicate the resonant electron wave functions of the associated resonant states. The error bars report the widths of the associated resonant states. Wave functions are plotted with contour values of ± 0.15 a.u.

cleavage, however, for serine 1, serine 2, and serine 4, the TNIs could decay through the C−OH bond cleavage at some specific resonances. Therefore the conformational effects are very important in the DEA process, which need to be considered in experimental and theoretical studies.

IV. CONCLUSION

In the present work, shape resonances of low-energy electron attachment to the four low-lying energy serine conformers and the subsequent dissociation dynamics have been studied by using quantum scattering method with the non-empirical model potentials in SCE. In the energy range of 0−10 eV, there are three shape resonances for serine 1, serine 2, and serine 4, and four shape resonances for serine 3. The resonant electron wave functions of the first resonant states for the four serine conformers are mainly localized on the COOH group with π^* anti-bonding character, renamed pseudo-π^* resonant states. The 1D dissociation dynamics along the $C_\alpha-C$, $C_\alpha-C_\beta$, $C_\alpha-N$, $C_\beta-OH$, and C−OH bonds stretching are investigated by calculating the total elec-

DOI:10.1063/1674-0068/30/cjcp1612228

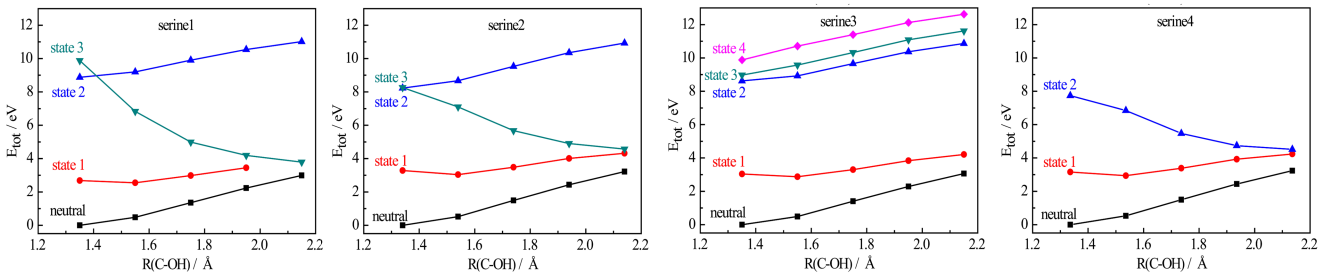

FIG. 11 Total electronic energy changes of the neutral and shape resonant states along the C−OH stretching coordinate for serine 1, serine 2, serine 3, and serine 4.

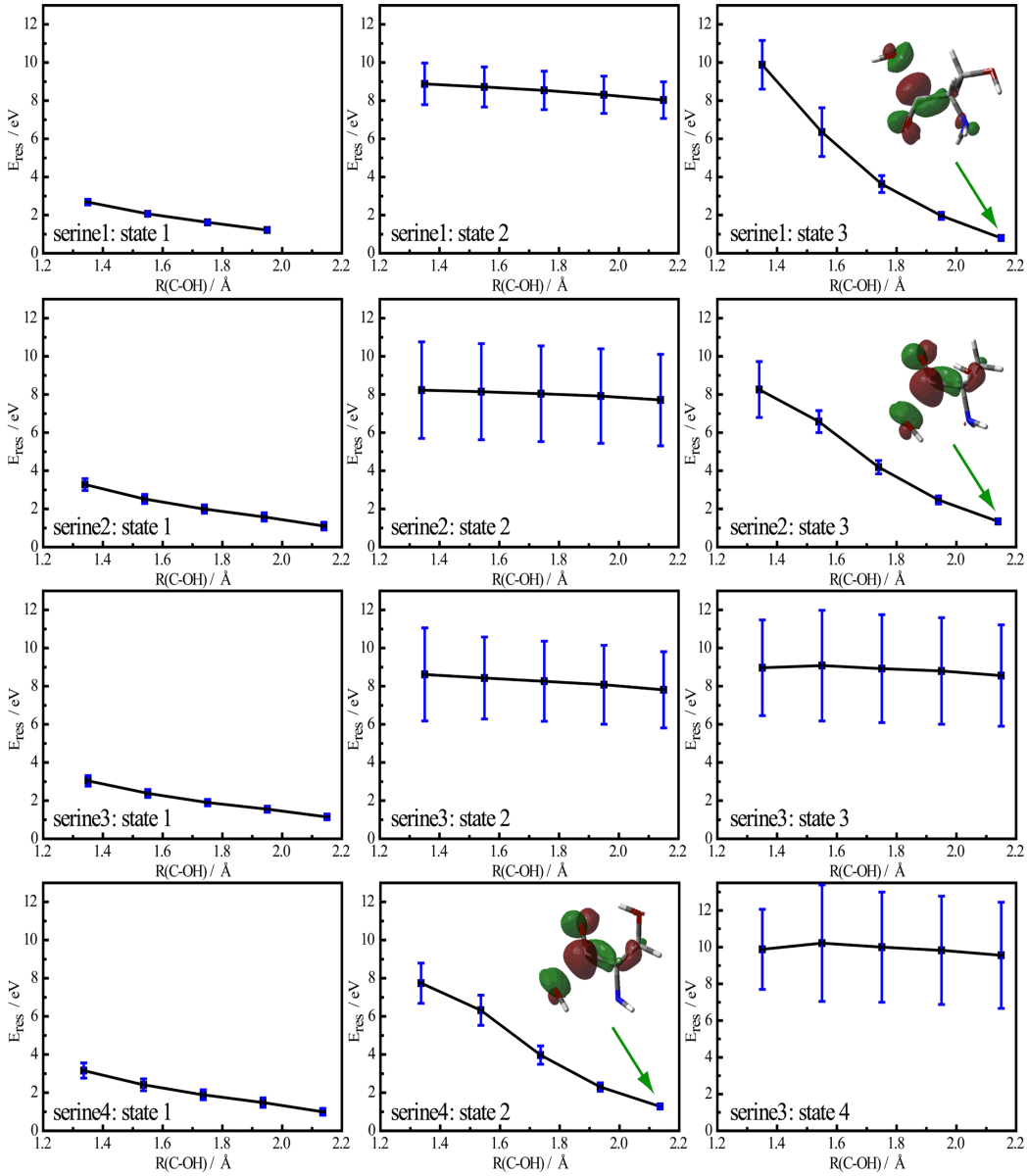

FIG. 12 Resonant energy changes of the shape resonant states along the C−OH stretching coordinate for serine 1, serine 2, serine 3, and serine 4. The insets indicate the resonant electron wave functions of the associated resonant states. The error bars report the widths of the associated resonant states. Wave functions are plotted with contour values of ±0.15 a.u.

DOI:10.1063/1674-0068/30/cjcp1612228

tronic energies and the resonant complex energies. The possible dissociation channels of partial fragments observed in recent DEA experiment [24] have been explained in the present work. The results of the 1D dissociation dynamics calculations indicate that the NH_2^- and O^- fragments with mass of 16 amu observed in the DEA experiment could coexist and the O^- fragment possibly comes from the side chain of serine. On the other hand, from the results of 1D dissociation dynamics calculation, a remarkable correlation between the different resonances and the specific bond cleavage were also found. For serine 1, the $C_\alpha-N$ or $C_\beta-OH$ bonds could be broken when the TNIs at resonant state 2, the $C_\alpha-C$ or $C-OH$ bonds could be broken when the TNIs at resonant state 3. For serine 2, the $C_\beta-OH$ bond could be broken when the TNIs at resonant state 2, the $C_\alpha-N$, $C_\alpha-C$, or $C-OH$ bonds could be broken when the TNIs at resonant state 3. For serine 3, the $C_\alpha-C$ or $C_\alpha-N$ bonds could be broken when the TNIs at resonant state 2, the $C_\beta-OH$ bond could be broken when the TNIs at resonant 3, the $C_\alpha-$ C_β bond could be broken when the TNIs at state 4. For serine 4, the $C_\alpha-N$, $C_\beta-OH$, or $C-OH$ bonds could be broken when the TNIs at state 2, the $C_\alpha-C$ could be broken when the TNIs at state 3. The bond-cleavage selectivity of the different resonant states for a certain conformer was also found in our former work on cysteine and cystine [47]. Moreover, conformational effect of serine on shape resonances and dissociative dynamics are found in present calculations. Therefore, the conformational effect may play very important roles in the ETS and DEA experiments on serine, since four low-lying conformers of serine coexist in the gas phase [45, 46].

V. ACKNOWLEDGMENTS

This work is supported by the National Natural Science Foundation of China (No.21303212 and No.21573209), the Ministry of Science and Technology of China (No.2013CB834602).

[1] B. Boudaïffa, P. Cloutier, D. Hunting, M. A. Huels, and L. Sanche, Science **287**, 1658 (2000).
[2] L. Sanche, Mass Spectrom. Rev. **21**, 349 (2002).
[3] F. Martin, P. D. Burrow, Z. L. Cai, P. Cloutier, D. Hunting, and L. Sanche, Phys. Rev. Lett. **93**, 068101 (2004).
[4] L. Sanche, Eur. Phys. J. D **35**, 367 (2005).
[5] I. Anusiewicz, M. Sobczyk, J. Berdys-Kochanska, P. Skurski, and J. Simons, J. Phys. Chem. A **109**, 484 (2005).
[6] J. Simons, Acc. Chem. Res. **39**, 772 (2006).
[7] R. Balog, J. Langer, S. Gohlke, M. Stano, H. Abdoul-Carime, and E. Illenberger, Int. J. Mass Spectrom. **233**, 267 (2004).
[8] I. Baccarelli, F. A. Gianturco, A. Grandi, N. Sanna, R. R. Lucchese, I. Bald, J. Kopyra, and E. Illenberger, J. Am. Chem. Soc. **129**, 6269 (2007).
[9] L. G. Christophorou, D. L. McCorkle and A. A. Christodoulides, *Electron-Molecule Interactions and Their Applications*, vol.1, L. G.Christophorou Ed, New York: Academic Press Inc., 477 (1984).
[10] K. Aflatooni, G. A. Gallup, and P. D. Burrow, J. Phys. Chem. A **102**, 6205 (1998).
[11] K. Aflatooni, B. Hitt, G. A. Gallup, and P. D. Burrow, J. Chem. Phys. **115**, 6489 (2001).
[12] S. Tonzani and C. H. Greene, J. Chem. Phys. **124**, 054312 (2006).
[13] F. A. Gianturco, F. Sebastianelli, R. R. Lucchese, I. Baccarelli, and N. Sanna, J. Chem. Phys. **128**, 174302 (2008).
[14] G. Hanel, B. Gstir, S. Denifl, P. Scheier, M. Probst, B. Farizon, M. Farizon, E. Illenberger, and T. D. Märk, Phys. Rev. Lett. **90**, 188104 (2003).
[15] S. Denifl, S. Matejcik, B. Gstir, G. Hanel, M. Probst, P. Scheier, and T. D. Märk, J. Chem. Phys. **118**, 4107 (2003).
[16] S. Denifl, S. Ptasińska, M. Probst, J. Hrušák, P. Scheier, and T. D. Märk, J. Phys. Chem. A **108**, 6562 (2004).
[17] A. M. Scheer, K. Aflatooni, G. A. Gallup, and P. D. Burrow, Phys. Rev. Lett. **92**, 068102 (2004).
[18] H. Abdoul-Carime, S. Gohlke, and E. Illenberger, Phys. Rev. Lett. **92**, 068103 (2004).
[19] D. Huber, M. Beikircher, S. Denifl, F. Zappa, S. Matejcik, A. Bacher, V. Grill, T. D. Märk, and P. Scheier, J. Chem. Phys. **125**, 084304 (2006).
[20] S. Denifl, P. Sulzer, D. Huber, F. Zappa, M. Probst, T. D. Märk, P. Scheier, N. Injan, J. Limtrakul, R. Abouaf, and H. Dunet, Angew. Chem. Int. Ed. **46**, 5238 (2007).
[21] Y. V. Vasil'ev, B. J. Figard, V. G. Voinov, D. F. Barofsky, and M. L. Deinzer, J. Am. Chem. Soc. **128**, 5506 (2006).
[22] P. Cloutier, C. Sicard-Roselli, E. Escher, and L. Sanche, J. Phys. Chem. B **111**, 1620 (2007).
[23] P. V. Shchukin, M. V. Muftakhov, J. Morr, M. L. Deinzer, and Y. V. Vasil'ev, J. Chem. Phys. **132**, 234306 (2010).
[24] J. Kočišek, P. Papp, P. Mach, Y. V. Vasil'ev, M. L. Deinzer, and Š. Matejčk, J. Phys. Chem. A **114**, 1677 (2010).
[25] F. A. Gianturco and R. R. Lucchese, J. Chem. Phys. **120**, 7446 (2004).
[26] A. Dora, J. Tennyson, L. Bryjko, and T. van Mourik, J. Chem. Phys. **130**, 164307 (2009).
[27] G. A. Gallup, P. D. Burrow, and I. I. Fabrikant, Phys. Rev. A **79**, 042701 (2009).
[28] F. A. Gianturco and R. R. Lucchese, New J. Phys. **6**, 66 (2004).
[29] F. A. Gianturco and R. R. Lucchese, J. Phys. Chem. A **108**, 7056 (2004).
[30] I. Baccarelli, A. Grandi, F. A. Gianturco, R. R. Lucchese, and N. Sanna, J. Phys. Chem. B **110**, 26240 (2006).
[31] M. Tashiro, J. Chem. Phys. **129**, 164308 (2008).
[32] C. Winstead and V. McKoy, J. Chem. Phys. **125**, 174304 (2006).
[33] C. Winstead and V. McKoy, J. Chem. Phys. **125**, 244302 (2006).
[34] C. Winstead, V. McKoy, and S. d'Almeida Sanchez, J.

DOI:10.1063/1674-0068/30/cjcp1612228

Chem. Phys. **127**, 085105 (2007).
[35] I. Baccarelli, F. Sebastianelli, F. A. Gianturco, and N. Sanna, Eur. Phys. J. D **51**, 131 (2009).
[36] T. P. M. Goumans, F. A. Gianturco, F. Sebastianelli, I. Baccarelli, and J. L. Rivail, J. Chem. Theory Comput. **5**, 217 (2009).
[37] C. Panosetti, I. Baccarelli, F. Sebastianelli, and F. A. Gianturco, Eur. Phys. J. D **60**, 21 (2010).
[38] Y. F. Wang and S. X. Tian, Phys. Chem. Chem. Phys. **13**, 6169 (2011).
[39] O. Plekan, V. Feyer, R. Richter, M. Coreno, G. Vall-llosera, K. C. Prince, A. B. Trofimov, I. L. Zaytseva, T. E. Moskovskaya, E. V. Gromov, and J. Schirmer, J. Phys. Chem. A **113**, 9376 (2009).
[40] V. Feyer, O. Plekan, R. Richter, M. Coreno, G. Vall-llosera, K. C. Prince, A. B. Trofimov, I. L. Zaytseva, T. E. Moskovskaya, E. V. Gromov, and J. Schirmer, J. Phys. Chem. A **113**, 5736 (2009).
[41] C. Pltzer and K. Kleinermanns, Phys. Chem. Chem. Phys. **4**, 4877 (2002).
[42] R. M. Balabin, Phys. Chem. Chem. Phys. **12**, 5980 (2010).
[43] R. M. Balabin, J. Phys. Chem. Lett. **1**, 20 (2010).
[44] M. E. Sanz, J. C. López, and J. L. Alonso, Phys. Chem. Chem. Phys. **12**, 3573 (2010).
[45] S. Blanco, M. E. Sanz, J. C. López, and J. L. Alonso, Proc. Natl. Acad. Sci. USA **104**, 20183 (2007).
[46] B. Lambie, R. Ramaekers, and G. Maes, J. Phys. Chem. A **108**, 10426 (2004).
[47] Y. F. Wang, S. X. Tian, and J. L. Yang, Phys. Chem. Chem. Phys. **13**, 15597 (2011).
[48] K. Takatsuka and V. McKoy, Phys. Rev. A **24**, 2473 (1981).
[49] R. R. Lucchese and F. A. Gianturco, Int. Rev. Phys. Chem. **15**, 429 (1996).
[50] J. P. Perdew and A. Zunger, Phys. Rev. B **23**, 5048 (1981).
[51] M. J. Frisch, G. W. Trucks, H. B. Schlegel, G. E. Scuseria, M. A. Robb, J. R. Cheeseman, G. Scalmani, V. Barone, B. Mennucci, G. A. Petersson, H. Nakatsuji, M. Caricato, X. Li, H. P. Hratchian, A. F. Izmaylov, J. Bloino, G. Zheng, J. L. Sonnenberg, M. Hada, M. Ehara, K. Toyota, R. Fukuda, J. Hasegawa, M. Ishida, T. Nakajima, Y. Honda, O. Kitao, H. Nakai, T. Vreven, J. A. Montgomery Jr., J. E. Peralta, F. Ogliaro, M. Bearpark, J. J. Heyd, E. Brothers, K. N. Kudin, V. N. Staroverov, R. Kobayashi, J. Normand, K. Raghavachari, A. Rendell, J. C. Burant, S. S. Iyengar, J. Tomasi, M. Cossi, N. Rega, J. M. Millam, M. Klene, J. E. Knox, J. B. Cross, V. Bakken, C. Adamo, J. Jaramillo, R. Gomperts, R. E. Stratmann, O. Yazyev, A. J. Austin, R. Cammi, C. Pomelli, J. W. Ochterski, R. L. Martin, K. Morokuma, V. G. Zakrzewski, G. A. Voth, P. Salvador, J. J. Dannenberg, S. Dapprich, A. D. Daniels, Ö. Farkas, J. B. Foresman, J. V. Ortiz, J. Cioslowski, and D. J. Fox, *Gaussian 09, Revision B.01*, Wallingford CT: Gaussian, Inc., (2009).
[52] S. Hara, J. Phys. Soc. Jpn. **22**, 710 (1967).
[53] S. Salvini and D. G. Thompson, J. Phys. B **14**, 3797 (1981).
[54] F. A. Gianturco, R. R. Lucchese, and N. Sanna, J. Chem. Phys. **100**, 6464 (1994).
[55] A. P. P. Natalense and R. R. Lucchese, J. Chem. Phys. **111**, 5344 (1999).
[56] H. Abdoul-Carime, S. Gohlke, and E. Illenberger, Phys. Chem. Chem. Phys. **6**, 161 (2004).

DOI:10.1063/1674-0068/30/cjcp1612228